Proceedings of IMECE2005
2005 ASME International Mechanical Engineering Congress and Exposition
November 5-11, 2005, Orlando, Florida USA

IMECE2005-79642

CONVECTIVE TRANSPORT IN AN OPTICAL FIBER COATING APPLICATOR FOR A NON-NEWTONIAN FLUID

Sang-Yeoun Yoo and Yogesh Jaluria
Department of Mechanical and Aerospace Engineering
Rutgers, The State University of New Jersey
Piscataway, New Jersey 08854
Email: jaluria@jove.rutgers.edu

ABSTRACT

Convective transport in an optical fiber coating applicator and die system has been simulated for a non-Newtonian fluid. Low density Polyethylene (LDPE) is employed for the numerical analysis, though ultraviolet (UV) curable acrylates are commonly used, because of lack of property information for acrylates and similar behavior of these two materials. The equations governing fluid flow and heat transfer are transformed to obtain flow in a cylindrical domain. A SIMPLE-based algorithm is used with a non-uniform grid. In contrast to the isothermal case, streamlines for the non-Newtonian fluid are found to be quite different for various fiber speeds. The temperature level in the applicator is much higher for the Newtonian case, due to the larger fluid viscosity and associated viscous dissipation. The shear near the fiber is found to be lower for the Newtonian fluid. As expected, the effects become larger with increasing fiber speed. A very high temperature rise is observed in the die, regardless of fiber speed. This study focuses on the non-Newtonian effects during the coating process, and several interesting and important features, as compared to the Newtonian case, are observed.

NOMENCLATURE

r	radial distance
z	axial distance
u	radial velocity
v	axial velocity
R	radius
H	height
$\vec{V}$	velocity vector
w	general velocity
ϕ	general variable
P	pressure
T	temperature
k	thermal conductivity
c_p	specific heat
μ	dynamic viscosity
ρ	density
τ	shear stress
$\dot{\gamma}$	shear rate
$\widetilde{\dot{\gamma}}$	rate of strain tensor
g	acceleration of gravity
$\vec{n}$	unit normal vector
$\vec{q}$	heat flux
n	power-law index

Subscript

f	fiber
in	inlet

INTRODUCTION

For a Newtonian fluid, the shear stress is proportional to the rate of shear. Most gases and liquids, with relatively small molecular weights, are known to be Newtonian [1]. However, many important industrial fluids, such as colloidal suspensions and polymeric solutions, show non-Newtonian behavior in their flow characteristics [1,2]. Non-Newtonian fluids are encountered in materials processing, such as food extrusion and optical fiber coating [3, 4]. Depending on the shear rate in the fluid, operating conditions, process parameters, and the previous history of the fluid, the fluid can be called pseudoplastic, dilatant, Bingham plastic, thixotropic, or rheopectic [1–6]. The last two categories, thixotropic and rheopectic, are time-dependent. For a pseudoplastic material (also called shear thinning material), such as ketchup and polymer solutions, an increase in the shear rate leads to a decrease in the apparent viscosity, which is the ratio of the shear stress to the shear rate. However, for a dilatant fluid

(also called shear thickening material), such as starch pastes, the viscosity increases with an increasing shear rate.

The shear rate at the fiber surface in the coating applicator and in the die has been found to be very high [7]. This high shear rate is detrimental to a proper coating. It is important to understand the fundamental aspects of the coating flow and of the associated heat transfer. In addition, many issues arise during the coating process, such as a bubble entrapment due to meniscus breakdown, instability and uniformity of the coating. However, it is important to determine when the coating fluid behaves as a non-Newtonian fluid and what triggers this behavior. For example, beading of coating occurs due to non-Newtonian effects, and this results in improper coating, which could ultimately lead to transmission loss [8]. Therefore, this study is directed at the fluid flow and heat transfer in the optical fiber coating applicator system for non-Newtonian fluids.

General methods for predicting properties of gases and liquids and their behavior in a given environment are described by Bretsznajder [9] and Reid [10]. Various numerical models for characterizing the rheology of Low Density Polyethylene (LDPE) are compared in the literature [11]. Chen et al. [11] proposed an empirical viscosity model for polymer melts, based on their experiments that considered the temperature effect on both flow behavior and the consistency index in a power-law model. The coefficients of the empirical model for LDPE and polypropylene (PP) were obtained from capillary rheometer measurements. Bird et al. [5] organized various non-Newtonian materials in terms of their characteristics. Numerous sample problems that can be encountered in polymer processing are solved. Properties of polymers and their fundamental behavior in polymer processing are also summarized by Tadmor and Gogos [6]. Jaluria [3] focussed on heat and mass transfer during the extrusion process for non-Newtonian materials such as plastics and food.

Not much work has been published in the open literature on the fiber coating process using a non-Newtonian material. Matallah et al. [14] used a time-stepping finite element method to study a tube-tooling wire-coating problem. A High-Density Polyethylene (HDPE) grade polymer was used for the simulation and modeled by a multi-mode Phan-Thien/Tanner (PTT) constitutive equation, which utilizes a single-mode solution to obtain a first approximate kinematics of the flow, to calculate each individual stress mode based on the frozen flow, and to make a correction on the kinematics. The focus was on the viscoelastic stresses arising in the coating process, and the flow geometry was varied to optimize the process by minimizing the induced stresses. Mutlu et al. [15] simulated the tube-tooling coating process for LDPE, using a finite element method similar to that of Matallah et al. [14]. Mutlu et al. [15] used a single-mode exponential PTT constitutive model, which is a transient network model to describe nonlinear flow phenomena [16].

Karwe and Jaluria [4] numerically studied the transport processes in a single-screw extruder for non-Newtonian materials. They employed the creeping flow approximation, so that the inertia terms in the momentum equations were neglected. The curvature effects were also neglected so that the screw channel was mathematically treated as unwound. It was found that the temperature variation of the barrel had a small effect on the corresponding velocity field. The flow was mainly governed by the dimensionless volumetric flow rate, which is generally called the throughput, emerging from the extruder. It was also found that strong viscous dissipation resulted in heat transfer from the fluid to the barrel in the downstream portion of the extruder. Lin and Jaluria [19] further investigated the flow and thermal fields in the single-screw extruder for non-Newtonian materials. The fluid and solid regions were solved to study conjugate heat transfer, and an iterative computational procedure was employed to match these solutions at the interface between the fluid and the barrel and the screw. It was found that the conjugate effects in the barrel were significant.

Wapperom and Hassager [13] used a finite element scheme to analyze a wire-coating process using Medium Density Polyethylene (MDPE). A copper wire was pulled with constant speed and the Carreau model was employed for the dependence of the viscosity on shear rate. The model consists of a zero-shear-rate viscosity, a power-law index and a time constant that determines the viscosity for low shear rates. A strong dependence on temperature is employed. The focus was on the thermal field, and the wire velocity, inlet temperature and power-law index were varied. Also varied were the properties of MDPE, with the specific heat and the thermal conductivity taken as linearly dependent on temperature. The wire diameter was taken as 1400 μm, and the annular die entrance was taken as 2000 μm, while the annular die exit was taken as 1100 μm. They found that the temperature rise was higher near the entrance and the die exit, due to large viscous dissipation. Therefore, the inlet temperature was found to be very important. A higher wire speed led to a much higher pressure drop, while the viscosity drastically decreased due to shear thinning and higher temperature.

Polymeric materials are commonly taken as generalized Newtonian fluid (GNF), due to the simplicity and robustness of this model [3, 5]. The idea is to incorporate the shear dependent viscosity into a Newtonian viscosity without causing any additional complexity. The shear stress can be written in general form as

$$\tau = -\mu\dot{\gamma} \tag{1}$$

where $\dot{\gamma}$ is the shear rate, which is related to the second invariant of the rate-of-strain tensor, $\widetilde{\dot{\gamma}}$, as [5]

$$\begin{aligned}\dot{\gamma} &= \sqrt{\frac{1}{2}\widetilde{\dot{\gamma}}\cdot\widetilde{\dot{\gamma}}} \\ &= \sqrt{\frac{1}{2}\sum_i\sum_j \dot{\gamma}_{ij}\dot{\gamma}_{ji}}\end{aligned} \tag{2}$$

Empirical models have been suggested for the relation between the shear stress and the shear rate, based on data fit of the experimental results. Examples include the power-law model, the Ellis model, and the Carreau model. For detailed descriptions of each model, see [3, 5, 6].

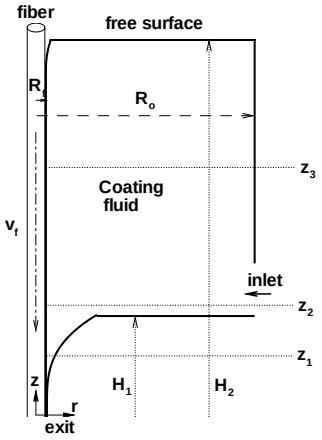

Figure 1. Schematic of a typical optical fiber applicator system

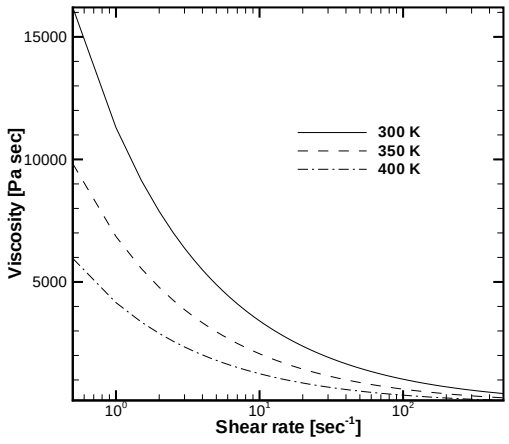

Figure 2. Viscosity variation of Low-Density Polyethylene (LDPE) with shear rates at different temperatures [4]

ANALYSIS

The schematic diagram of a typical optical fiber coating system is shown in Figure 1. Axisymmetric, non-Newtonian, flow and heat transfer are assumed and the appropriate cylindrical coordinates are shown. LDPE is selected for the coating material to identify non-Newtonian fluid behavior, since its material properties are well-established [4–6, 11, 17]. The viscosities of this material at three temperatures are shown in Figure 2. As is explained in detail later, the viscosity depends on both the shear rate and temperature of the flow. It becomes smaller as either the shear rate or temperature increases. All the properties, except density, are taken as variable, since the density of most polymer melts stays fairly constant at typical changes in pressure [19].

Governing Equations

As mentioned earlier, governing equations for incompressible axisymmetric fluid flow and heat transfer in steady state are solved. Thus, the continuity equation is

$$\frac{1}{r}\frac{\partial}{\partial r}(\rho r u)+\frac{\partial}{\partial z}(\rho v)=0 \tag{3}$$

Unlike a Newtonian fluid, the viscosity is not constant with change in shear stress. Therefore, the equation for the conservation of the momentum becomes [12]

$$\rho\left(u\frac{\partial w_\phi}{\partial r}+v\frac{\partial w_\phi}{\partial z}\right)=-\frac{\partial P}{\partial \phi}+\left[\frac{1}{r}\frac{\partial}{\partial r}\left(r\tau_{r\phi}\right)+\frac{\tau_{z\phi}}{\partial z}\right]+\rho g_\phi \tag{4}$$

where ϕ represents a general variable, with the corresponding variables given as

$$\phi=\begin{bmatrix} r \\ z \end{bmatrix},\ w_\phi=\begin{bmatrix} u \\ v \end{bmatrix},\ g_\phi=\begin{bmatrix} 0 \\ g_z \end{bmatrix}$$

Considering variable thermal properties, the energy equation for the coating fluid becomes

$$\rho c_p\left(u\frac{\partial T}{\partial r}+v\frac{\partial T}{\partial z}\right)=\left[\frac{1}{r}\frac{\partial}{\partial r}\left(kr\frac{\partial T}{\partial r}\right)+\frac{\partial}{\partial z}\left(k\frac{\partial T}{\partial z}\right)\right] +\tau_{rr}\frac{\partial u}{\partial r}+\tau_{zz}\frac{\partial v}{\partial z}+\tau_{rz}\left(\frac{\partial v}{\partial r}+\frac{\partial u}{\partial z}\right) \tag{5}$$

where the shear stresses are as follows;

$$\begin{aligned}\tau_{rr}&=2\mu\frac{\partial u}{\partial r}\\ \tau_{zz}&=2\mu\frac{\partial v}{\partial z}\\ \tau_{rz}&=2\mu\left(\frac{\partial v}{\partial r}+\frac{\partial u}{\partial z}\right)\end{aligned} \tag{6}$$

All the governing equations, (3) - (6), for a complex geometry are then transformed to a simple cylindrical domain. For a detailed description of the transformation, see [7].

For the current 2-D axisymmetric coordinates, equation (1) has a shear rate, which is given by

$$\dot{\gamma}=\sqrt{\frac{1}{2}\left[4(\frac{\partial u}{\partial r})^2+2(\frac{\partial u}{\partial z}+\frac{\partial v}{\partial r})^2+4(\frac{u}{r})^2+4(\frac{\partial v}{\partial z})^2\right]} \tag{7}$$

All the terms in the physical grid are transformed to simple cylindrical domain for easier computation [7]. The constitutive equa-

Table 1. Wire-grade LDPE used for the calculations [4]

Property	LDPE
Density ρ [kg/m^3]	750
Reference dynamic viscosity μ_o [Ns/m^2]	2000
Reference thermal conductivity k_o [W/mK]	0.3
Reference specific heat coefficient c_o [J/kgK]	2570
Temperature coefficient of viscosity b [$^oC^{-1}$]	0.01
Power law index n	0.48
Reference strain rate γ_o [s^{-1}]	1.0

tion for the viscosity finally becomes

$$\mu = \mu_o \left(\frac{\dot{\gamma}}{\dot{\gamma}_o} \right)^{n-1} e^{-b(T-T_o)} \tag{8}$$

The coefficients used in the equation and the reference materials properties are shown in Table 1.

Boundary Conditions

A fiber is moving at the center of the applicator at a given speed, as seen in Figure 1. The temperature distribution at the fiber is calculated from the energy conservation and is denoted by $T_f(z)$ [7]. The boundary conditions used for this study can be written as

$$r = R_f\ ; \quad u = 0,\ v = v_f,\ T = T_f(z) \tag{9}$$
$$r = R_o\ ; \quad u = 0,\ v = 0,\ \vec{q}\cdot\vec{n} = 0 \tag{10}$$
$$z = H_1\ ; \quad u = 0,\ v = 0,\ T = T_{in} \tag{11}$$
$$z = H_2\ ; \quad \vec{V}\cdot\vec{n} = 0,\ \vec{q}\cdot\vec{n} = 0 \tag{12}$$
$$z = 0\ ; \quad u = 0,\ \frac{\partial v}{\partial z} = 0,\ \frac{\partial T}{\partial z} = 0 \tag{13}$$

At the fluid inlet, the vertical velocity is taken as zero, temperature is given as T_{in} and the radial velocity, u_{in}, is calculated from the mass flow rate at the die exit. The applicator bottom wall and the top surface are located at $z = H_1$ and $z = H_2$, respectively, as seen in Figure 1. At the die wall, the no-slip boundary condition is used. In order to investigate the effect of thermal conditions outside the die wall, the heat transfer coefficient is separately varied. At the top surface in the applicator, $z = H_2$, a free surface condition is used, since a no-slip boundary condition in the region has been found to yield higher shear rates along the fiber [7].

Material Properties

Practically, a material exhibiting non-Newtonian behavior is very complicated to be modeled. This complexity can be increased largely due to the shear rate in the fluid, operating conditions, process parameters, or the previous history of the fluid. Although UV-curable acrylates are typically used as coating material for optical fibers, a lack of property information and the use of LDPE for metal wires led to the choice of LDPE for modeling of the flow and heat transfer. As explained earlier, much effort has been directed at characterizing the non-Newtonian fluid behavior of LDPE. Thus, LDPE is selected for the current study.

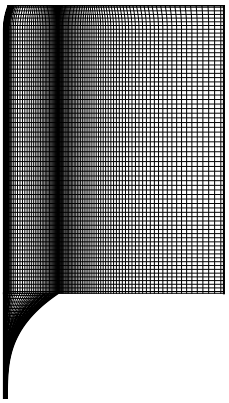

Figure 3. Typical numerical grid used in the calculations

It is assumed that the thermal conductivity for LDPE depends on temperature. The corresponding equation employed is

$$k = a_k(1.0 + b_k(T - 297.5)) \tag{14}$$

where a_k is the thermal conductivity at a reference temperature, T_o, and b_k is a coefficient. For the current study, a_k=0.3 and b_k=-0.0005 are used, since typical values of b_k for liquids ranges from -0.0005 to -0.0002 [10].

The specific heat for LDPE is also taken as temperature-dependent, i.e.,

$$c_p = a_c(1.0 + b_c(T - 423.0)) \tag{15}$$

where a_c is the specific heat at the reference temperature, and b_c is a coefficient. For the current study, $a_c = 2570$ and $b_c = 0.001$ are adopted from Wapperom and Hassager [13].

Numerical Modeling

The conservation equations governing fluid flow and heat transfer are transformed to be solved on a cylindrical domain [7]. Non-uniform grids are generated, with smaller grids in regions where high gradients are expected. For example, a very fine grid is constructed near the fiber surface, since the shear rate near the region has been found earlier to be very high [7]. A typical numerical mesh used for the calculation is shown in Figure 3. Many cases were tested to ensure grid independency, and 110×70 is

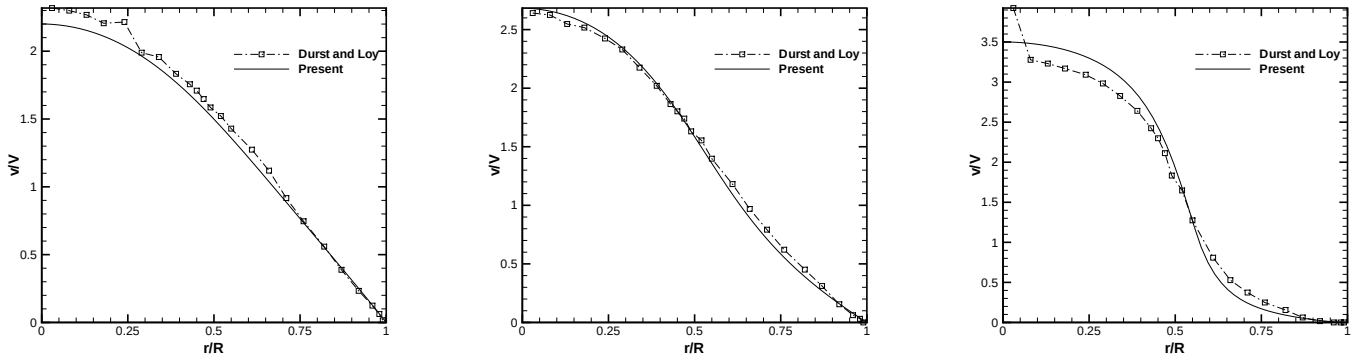

(a) At z/D=0.261 (b) At z/D=0.157 (c) At z/D=0.052

Figure 4. Comparisons of calculated axial velocities, for Re=196, at three downstream locations, with experimental results by Durst and Loy [18]

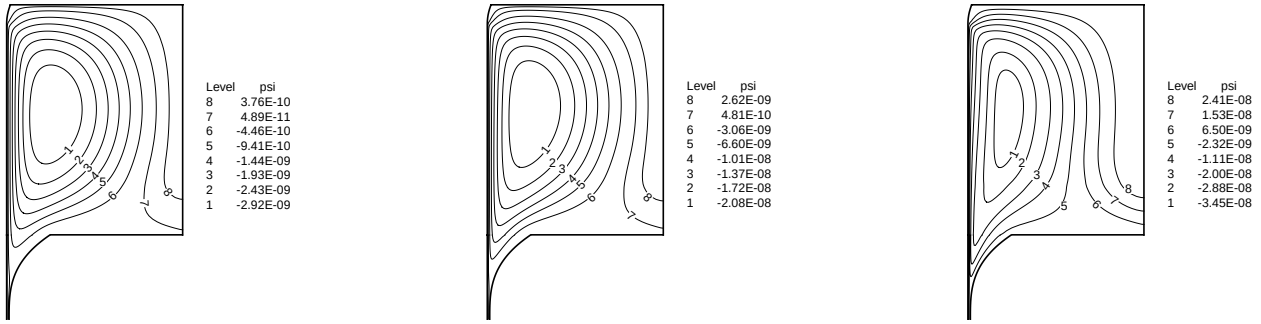

(a) v_f=0.1 m/sec (b) v_f=1m/sec (c) v_f=5m/sec

Figure 5. Comparisons of streamlines at various fiber speeds for n=0.48

chosen for the applicator while 50×120 for the die, both in (r,z).

A SIMPLE-based algorithm was developed to model the optical fiber coating process [20]. The pressure field is initially guessed and then updated at each iteration, based on the velocity field that was calculated from the previous iteration. The calculation continues until the pressure and the temperature fields are unchanged. The following convergence criterion is adopted

$$\varepsilon = max \left| \frac{\phi_{i,j}^{new} - \phi_{i,j}^{old}}{\phi_{i,j}^{old}} \right| \qquad (16)$$

where ϕ is a general variable, which can be P or T. The calculations are stopped when ε_P and ε_T are less than 3×10^{-4} and 1×10^{-5}, respectively. These values were varied to ensure that the results are independent of the values chosen.

Numerous cases have been tested to validate the code used. Durst and Loy [18] measured a velocity in a pipe with a sudden contraction in its cross sectional area. This experiment setup is very well suited for comparison with the current numerical simulation since the geometries are very similar and the diameter at the coating die entrance is typically much smaller than that of an applicator. Three downstream locations are selected to see the flow structure near the contraction, which starts at z/D=0. The higher the value of z/D, the closer it is to the flow inlet. Figure 4 shows that the two results match very well. A fully developed flow near the entrance is seen to approach the smaller pipe, as seen in Figure 4 (a), and the centerline velocity starts increasing, as seen in Figure 4 (b). A sudden reduction in area and a transfer of momentum from the outer region to the inner one resulted in the bulge at the center, as seen in Figure 4 (c). This comparison indicates the validity of the current simulation.

RESULTS AND DISCUSSION

Figure 5 shows the streamlines at various fiber speeds for power-law index, n, of 0.48. In contrast to the isothermal cases, where the pattern of streamlines was similar regardless of fiber speed, the streamlines for the non-Newtonian fluid are found to be different for various fiber speeds [7]. As the fiber speed increases, the circulation in the applicator becomes stronger. Near the fiber surface, the flow accelerates for all fiber speeds. It is

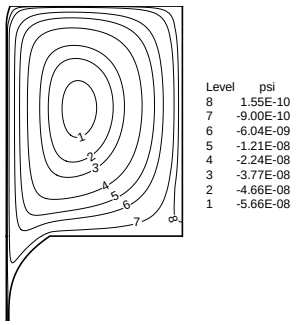

(a) v_f=0.1 m/sec

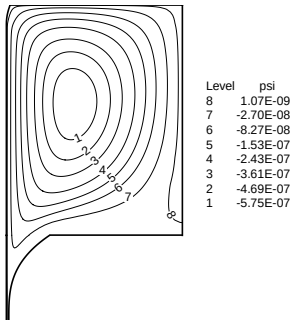

(b) v_f=1m/sec

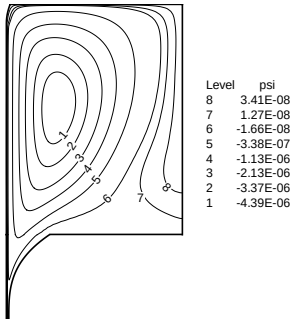

(c) v_f=5m/sec

Figure 6. Comparisons of streamlines at various fiber speeds for n=1.0

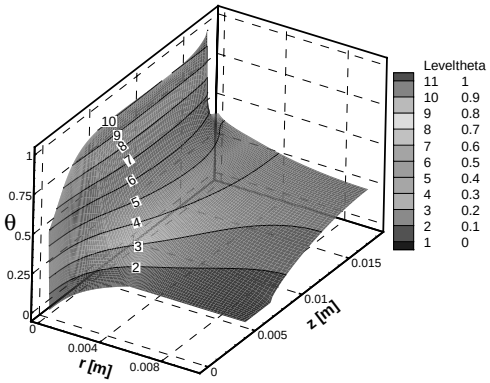

(a) n=0.48

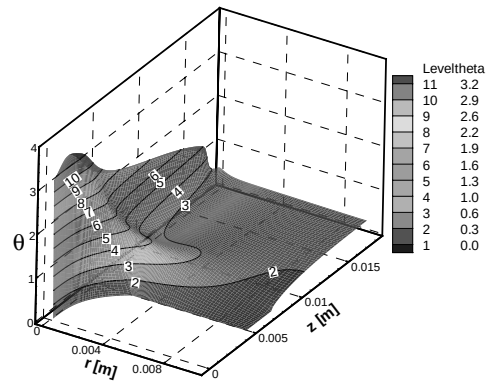

(b) n=1

Figure 7. Isotherms for Newtonian and non-Newtonian fluids at a fiber speed of 0.1m/s

also seen that the circulation becomes distorted as the fiber speed increases. This is related to the non-uniform thermal field and a relatively inadequate modeling in the low shear rate regions, associated with the power-law fluid model. Thus, the modified power-law model can be used to improve the current model since it allows the apparent viscosity to become a constant at low shear rates [3].

When the Newtonian fluid is employed, i.e., n=1.0, the flow field is found to be slightly different from that for the non-Newtonian fluid, as seen in Figure 6. As the fiber speed increases, the flow pattern remains similar, but the strength of the circulation becomes higher for Newtonian fluids than that for non-Newtonian fluids. This is due to the larger fluid viscosity for n=1.0. The flow is shown to accelerate moderately near the fiber surface, as compared to Newtonian flow. This is due to the non-uniform thermal field that results in non-uniform viscosity, such that shear near the region is lower for the Newtonian fluid. This will be discussed in detail later.

As the fiber speed increases, the temperature level was found to increase due to the corresponding increase in viscous dissipation [22]. Wapperom and Hassager [13] also found severe temperature rise near the entrance and the die exit, due to strong viscous dissipation. Figure 7 shows the temperature contours for both Newtonian and non-Newtonian fluids at low fiber speed. For n=0.48, the temperature near the fiber was higher than that in the remaining region, both in the applicator and in the fiber. However, for n=1.0, the temperature in the die started increasing and reached a maximum in the die. The fiber temperature is also found to increase as it travels toward the die exit. For a non-Newtonian fluid, the rising temperature and the high shear both

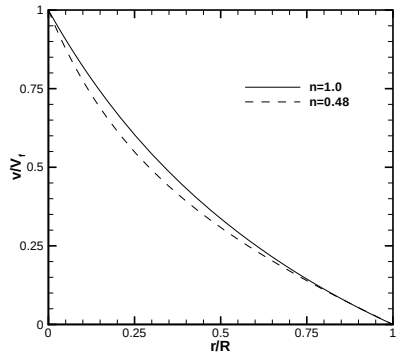

(a) v_f=0.1 m/sec

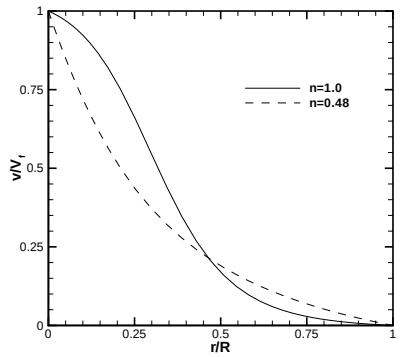

(b) v_f=1m/sec

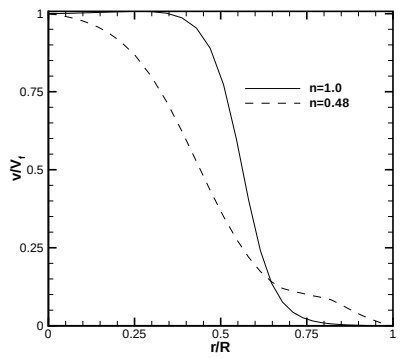

(c) v_f=5m/sec

Figure 8. Axial velocity profiles at the die exit for Newtonian and non-Newtonian fluids at different fiber speeds

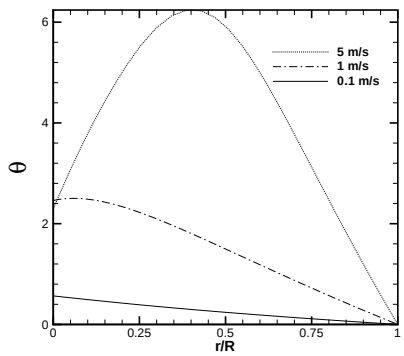

(a) At z=z1

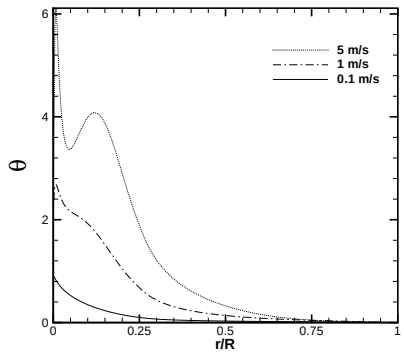

(b) At z=z2

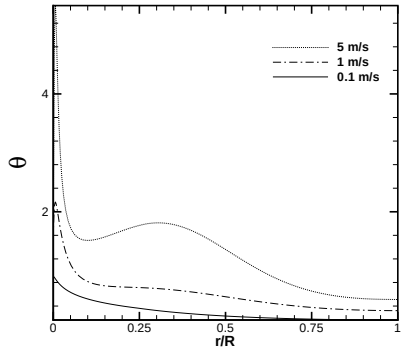

(c) At z=z3

Figure 9. Comparisons of temperature distributions at various axial locations for n=0.48

lead to a decrease in the viscosity, according to equation (8).

The axial velocity profiles at the die exit for both Newtonian and non-Newtonian fluids are compared with each other and shown in Figure 8. The solid line is for a Newtonian fluid while the dotted line is for a non-Newtonian fluid. It is found that the non-Newtonian flow effects become clearer as the fiber speed increases. At low fiber speed, the two profiles are quite close to each other, as explained earlier. However, with increasing fiber speed, the difference between the two profiles becomes higher. This is due to the low shear near the fiber for the Newtonian fluid. The shear is found to become even lower with higher fiber speeds. This low shear at higher fiber speed is seen as a longer flat profile in the radial direction near the fiber, at r/R=0.

The temperature profiles at various axial locations are shown in Figure 9. As the fiber speed increases, the temperature level is also found to increase accordingly. The temperature rise is larger at higher fiber speed. As one moves from the fiber entrance to-

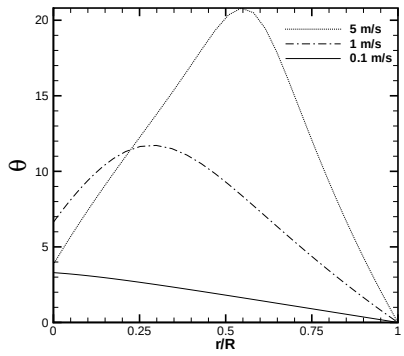

(a) At z=z1

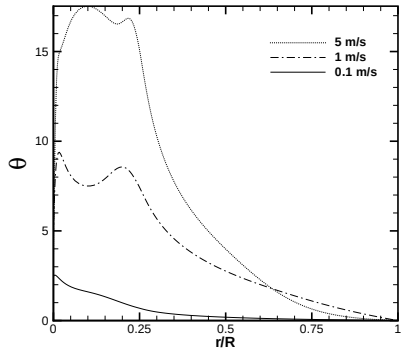

(b) At z=z2

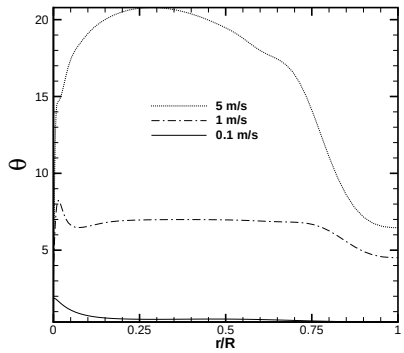

(c) At z=z3

Figure 10. Comparisons of temperature distributions at various locations for n=1

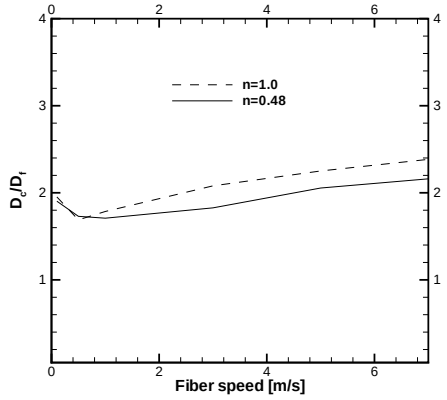

(a) coating thickness

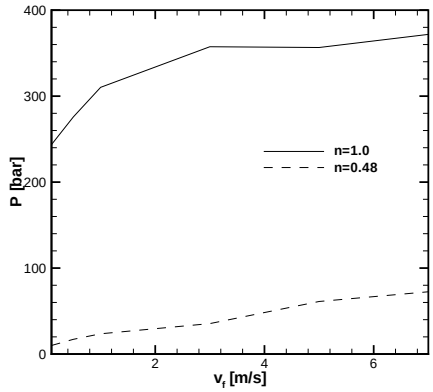

(b) maximum pressure

Figure 11. Effect of fiber speed on coating thickness and maximum pressure in the die

ward the die exit, which is from $z = z_3$ to $z = z_1$, the temperature rise in the die becomes higher. Therefore, the fluid in the die starts heating the fiber, as seen in the change of the direction of the temperature gradient at the fiber surface at r/R=0 in Figure 9 (a). A stronger circulation at higher fiber speed and the flow rejoining the circulation from the die entrance are responsible for a kink near the fiber in Figure 9 (b).

The temperature profiles at three axial locations for n=1 are seen in Figure 10. When the shear effect is excluded from the constitutive equation (8), for the viscosity of LDPE, that is at n=1, similar results are obtained in the die at $z = z_1$. However, a noticeable difference is the temperature level arises in both the applicator and the die. The temperature level in the applicator is much higher for the Newtonian case, so that the fluid in the applicator constantly heats up the fiber as it moves from the fiber entrance to the die exit. This is seen in the positive temperature gradient at r/R=0, the gradient being equivalent to a heat flux to the fiber. This is due to the stronger viscous dissipation associated with higher fiber speed. This high temperature rise and the corresponding heating near the die exit was also observed by Karwe and Jaluria [4] and by Wapperom and Hassager [13].

The fiber speed was found to be of critical importance during the fiber coating process [7, 8, 13]. When the speed is increased, the corresponding viscous dissipation becomes higher so that it leads to a increase in the temperature level. This rise of temperature level results in a non-uniform thermal field so that it also affects the flow field, and vice versa. Hence, this interaction eventually can affect the final coating thickness. Figure 11 shows the effect of the fiber speed on the final coating thickness and on the maximum pressure in the die, respectively. It is found that

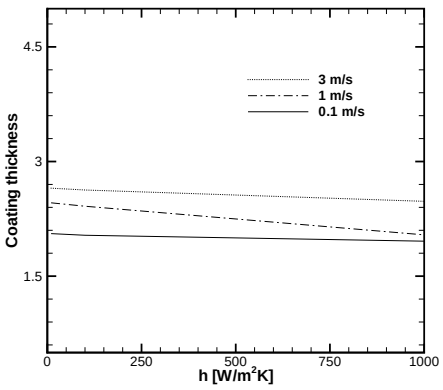

(a) n=0.48

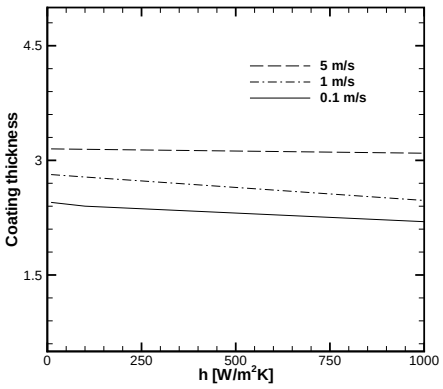

(b) n=1.0

Figure 12. Effects of thermal conditions outside the die wall on coating thickness

non-Newtonian fluid effects are insignificant, as far as the coating thickness is concerned. However, the localized maximum pressure in the die is found to be greatly affected by the non-Newtonian behavior. The pressure field shows a significant difference between Newtonian and non-Newtonian fluids. At n=1, the pressure is found to be much higher than that at n=0.48. As seen in Figure 11 (b), both maximum pressures increase linearly with the fiber speed. It should be noted that these high localized pressures should be avoided, since it inhibits proper wetting and degrades the fiber strength [21].

The effect of thermal conditions outside the applicator during the coating process was found to be insignificant [22]. This study varied the thermal conditions outside the die wall by changing the convective heat coefficient, h, from 0 to 1000 W/m^2K for a fixed adiabatic applicator wall. Practically, this is equivalent either to cooling the die wall by surrounding it with a cold jacket or to blowing a cooler fluid around the die wall. The effect of h on the final coating thickness for both n=0.48 and n=1 is shown in Figure 12. It is found that the coating thickness for n=1 is a little higher than that for n=0.48, but the overall behavior for all the fiber speeds is similar.

CONCLUSIONS

The convective transport in an optical fiber coating applicator and a die system has been simulated for a non-Newtonian fluid. LDPE is employed for the coating fluid, due to a lack of property information for UV-curable acrylates, which are commonly used. Geometric and temporal effects are not included in this study in order to focus on non-Newtonian effects. Variable properties are used to investigate the effect of non-Newtonian behavior on the fluid flow and heat transfer, whereas the density is kept constant. A Generalized Newtonian fluid is adopted for the constitutive equation.

In contrast to the isothermal cases, where the pattern of streamlines was similar regardless of fiber speed, the streamlines for non-Newtonian fluids are found to be different at various fiber speeds. Near the fiber surface, the flow accelerates for all fiber speeds, the acceleration being higher for the non-Newtonian fluid. The strength of the circulation becomes higher for the Newtonian fluids than that for the non-Newtonian fluids due to larger viscosity of the former. The temperature level in the applicator is much higher for this Newtonian case, so that the fluid in the applicator constantly heats up the fiber as it moves from the fiber entrance to the die exit. For an increasing fiber speed, the difference between the two die exit profiles becomes larger. This is due to the low shear near the fiber for a Newtonian fluid. As far as the coating thickness is concerned, non-Newtonian fluid effects are found to be insignificant. At n=1, the pressure is found to be much higher than that for n=0.48. The thermal conditions outside the die wall are also found to be insignificant. This study is directed at the non-Newtonian effects during the coating process and many interesting results have been presented. However, a further study is required for a complete analysis to optimize the quality of the coating, die design, and production rate for typical coating fluids.

ACKNOWLEDGMENT

The authors acknowlege the support by National Science Foundation, under grant No. CTS-0119356, for this work and the discussions with Prof. C. E. Polymeropoulos.

REFERENCES

[1] Wilkinson, W.L., 1960, "Non-Newtonian fluids: fluid mechanics, mixing and heat transfer," Pergamon press ltd., Headington Hill Hall, Oxford

[2] Irvine, T.F. and Karni, J., 1987, "Non-Newtonian fluid flow and heat transfer," In Handbok of single-phase convective heat transfer (Kakac, S., Shah, R.K., and Aung, W., ed.) Chapter 20, pp20.1-20.57, A Wiley-Interscience publication, Canada

[3] Jaluria, Y., 1996, "Heat and mass transfer in the extrusion of non-Newtonian materials," Advances in heat transfer, vol. 28, pp145-230

[4] Karwe, M. and Jaluria, Y., "Numerical simulation of fluid flow and heat transfer in a single-screw extruder for non-Newtonian fluids," Numerical heat transfer, Part A., v. 17, pp. 167-190, 1990

[5] Bird, R.B., Armstrong, R.C., and Hassager, O., "Dynamics of polymeric liquids," John Wiley and Sons, 2nd ed., v.1, 1987
[6] Tadmor, Z. and Gogos, C., 1979, "Principles of polymer processing," John Wiley and Sons, Inc.
[7] Yoo, S.Y. and Jaluria, Y., 2005, "Isothermal flow in an optical fiber coating applicator and die system,", submitted
[8] Paek,U.C, "High-speed High-strength fiber drawing," Journal of lightwave technology, vol LT-4, n8, p1048-1060, 1986
[9] Bretsznajder, S., 1971, "Prediction of transport and other physical properties of fluids," Pergamon press ltd., Headington Hill Hall, Oxford
[10] Reid, R., and Sherwood, T., 1966, "The properties of gases and liquids," MaGraw-Hill, Inc., 2nd ed.
[11] Chen, Z., Chao, P., and Chiu, S., 2003, "Empirical viscosity model for polymers with power-law flow behavior," Journal of applied polymer science, v.88, pp. 3045-3057
[12] Burmeister, L.C., 1993, "Convective heat transfer," John Wiley and Sons, Inc., 2nd ed., New York, NY
[13] Wapperom, P. and Hassager, O., 1999, "Numerical simulation of wire-coating: the influence of temperature boundary conditions," Polymer engineering and science, **39**, pp. 2007-2018
[14] Matallah, H., Townsend, P., and Webster,M. F., 2000, "Viscoelastic multi-mode simulations of wire-coating," v. 90 (**2**), pp. 217-241
[15] Mutlu,I., Townsend, P. and Webster, M. F., 1998, "Simulation of cable-coating viscoelastic flows with coupled and decoupled schemes," v.78 (**1**), pp.1-23
[16] Wientjes, R.H.W., Jongschaap, R.J.J., Duits, M.H.G. and Mellema, J., "A new transient network model for associative polymer networks," J. Rheol. 43(2), March/April 1999, pp375-391
[17] Fenner, R., 1979, "Principles of polymer processing," The Macmillan press Ltd.
[18] Durst,F. and Loy, T., "Investigation of laminar flow in a pipe with sudden contraction of cross sectional area," Computers and Fluids, v.13, n.1, p15-36, 1985
[19] Lin, P. and Jaluria, Y., "Conjugate thermal transport in the channel of an extruder for non-Newtonian fluids," International Journal of Heat and Mass Transfer 41, pp. 3239-3253, 1998
[20] Patankar, S.V., 1980, "Numerical Heat Transfer and Fluid Flow", Taylor and Francis
[21] Paek,U.C, "Free drawing and polymer coating of silica glass optical fibers," Journal of Heat transfer, v121, p774-788, 1999
[22] Yoo, S.Y. and Jaluria, Y., 2005, "Conjugate Heat Transfer in an Optical Fiber Coating Process" ASME Summer Heat Transfer Conference, San Francisco, California